

# A simulation-optimization methodology to model urban catchments under non-stationary extreme rainfall events.

Jato-Espino, D, Sillanpaa, N, Charlesworth, S & Rodriguez-Hernandez, J

Author post-print (accepted) deposited by Coventry University's Repository

**Original citation & hyperlink:**

Jato-Espino, D, Sillanpaa, N, Charlesworth, S & Rodriguez-Hernandez, J 2017, 'A simulation-optimization methodology to model urban catchments under non-stationary extreme rainfall events.' *Environmental Modelling & Software*, vol (in press), pp. (in press).

<https://dx.doi.org/10.1016/j.envsoft.2017.05.008>

DOI [10.1016/j.envsoft.2017.05.008](https://dx.doi.org/10.1016/j.envsoft.2017.05.008)

ISSN 1364-8152

ESSN 1873-6726

Publisher: Elsevier

**NOTICE: this is the author's version of a work that was accepted for publication in *Environmental Modelling & Software*. Changes resulting from the publishing process, such as peer review, editing, corrections, structural formatting, and other quality control mechanisms may not be reflected in this document. Changes may have been made to this work since it was submitted for publication. A definitive version was subsequently published in *Environmental Modelling & Software*, (2017) DOI: [10.1016/j.envsoft.2017.05.008](https://dx.doi.org/10.1016/j.envsoft.2017.05.008)**

© 2017, Elsevier. Licensed under the Creative Commons Attribution-NonCommercial-NoDerivatives 4.0 International

<http://creativecommons.org/licenses/by-nc-nd/4.0/>

Copyright © and Moral Rights are retained by the author(s) and/ or other copyright owners. A copy can be downloaded for personal non-commercial research or study, without prior permission or charge. This item cannot be reproduced or quoted extensively from without first obtaining permission in writing from the copyright holder(s). The content must not be changed in any way or sold commercially in any format or medium without the formal permission of the copyright holders.

This document is the author's post-print version, incorporating any revisions agreed during the peer-review process. Some differences between the published version and this version

may remain and you are advised to consult the published version if you wish to cite from it.

# A simulation-optimization methodology to model urban catchments under non-stationary extreme rainfall events

**Daniel Jato-Espino<sup>1</sup>; Nora Sillanpää<sup>2</sup>; Susanne M. Charlesworth<sup>3</sup>; Jorge Rodriguez-Hernandez<sup>4</sup>**

<sup>1,4</sup> GITECO Research Group, Universidad de Cantabria, Av. de los Castros s/n, 39005, Santander, Spain

<sup>2</sup> Department of Built Environment, Aalto University School of Engineering, P.O. Box 15200, Aalto, Finland

<sup>3</sup> Centre for Agroecology, Water and Resilience (CAWR), Coventry University, CV1 5FB, Coventry, United Kingdom

E-mail addresses: [jatod@unican.es](mailto:jatod@unican.es) (D. Jato-Espino); [nora.sillanpaa@aalto.fi](mailto:nora.sillanpaa@aalto.fi) (N. Sillanpää); [apx119@coventry.ac.uk](mailto:apx119@coventry.ac.uk) (S. M. Charlesworth); [rodrih@unican.es](mailto:rodrih@unican.es) (J. Rodriguez-Hernandez);

\* Corresponding author. Tel.: +34 942203943; Fax: +34 942201703.

## Abstract

Urban drainage is being affected by Climate Change, whose effects are likely to alter the intensity of rainfall events and result in variations in peak discharges and runoff volumes which stationary-based designs might not be capable of dealing with. Therefore, there is a need to have an accurate and reliable means to model the response of urban catchments under extreme precipitation events produced by Climate Change. This research aimed at optimizing the stormwater modelling of urban catchments using Design of Experiments (DOE), in order to identify the parameters that most influenced their discharge and simulate their response to severe storms events projected for Representative Concentration Pathways (RCPs) using a statistics-based Climate Change methodology. The application of this approach to an urban catchment located in Espoo (southern Finland) demonstrated its capability to optimize the calibration of stormwater simulations and provide robust models for the prediction of extreme precipitation under Climate Change.

## Keywords

Climate Change; Design of Experiments; Geographic Information System; Stormwater modelling; Urban hydrology.

# 1. Introduction

Urban growth during the second half of the 20<sup>th</sup> century exacerbated deficiencies in terms of rainwater drainage and led to increased flooding and diffuse pollution ([Bayon et al., 2015](#)). Urban development upstream of a catchment alters its inflow hydrograph increasing runoff volume and flow ([Sloat and Hwang, 1989](#)), whilst the time elapsed from the onset of rainfall until peak flow (i.e. the time of concentration) decreases. This results in water being conveyed and discharged more rapidly than happens naturally ([Perales-Momparler et al., 2015](#)). Traditionally, drainage systems capture water to minimize runoff accumulation and then quickly transfer it to a sewer network formed of a series of connected pipes and manholes. However, urbanization results in a series of hydrological alterations whose impact often exceeds the capacity of these systems. Nordic countries like Finland are particularly struggling to cope with these alterations, which include earlier spring snowmelt and increased runoff depths and peak flows ([Valtanen et al., 2014](#); [Siljanpää and Koivusalo, 2015](#)).

Furthermore, the effect of urban development on drainage is expected to be aggravated by Climate Change (CC), due to its potential impact on rainfall. Although no global trends have been detected so far in this respect and the projected changes in different regions do not follow the same directions ([IPCC, 2007](#); [Zhang et al., 2007](#)), precipitation has increased at high latitudes due to changing climate ([IPCC, 2007](#)). Consequently, no global evidence has been found in relation to the impact of CC on flood frequency ([Kundzewicz and Schellnhuber, 2004](#); [Huntington, 2006](#)), but positive trends in winter and spring discharge have been reported in Nordic countries ([Wilson et al., 2010](#)), as well as increases in annual discharge at regional scales in south-western Norway and northern Sweden ([Lindström and Bergström, 2004](#)). Furthermore, [Korhonen and Kuusisto \(2010\)](#) identified earlier spring peak flows and clear increases in winter and spring discharge in Finland.

Due to their complex interactions with drainage patterns, both urbanization and CC have been addressed in the literature with the support of numerical models to simulate water and climate-related processes. Stormwater models emerged in the early 1970s to facilitate the simulation and analysis of hydrological processes in urban catchments ([Whipple et al., 1982](#)). These models can be classified into different groups according to input management (deterministic or stochastic), physical foundations (conceptual or empirical), simulation (event or continuous), spatial variability (distributed or lumped), infiltration (physical, empirical or hydrological) and routing (hydrological, hydraulic, empirical or statistical) ([Zoppou, 2001](#)). General Circulation Models (GCMs) have been developed by different research centers worldwide ([IPCC, 2007](#)) to simulate and project climate processes. However, since the impact of such processes is expected to occur at more regional

scales ([Giorgi et al., 2009](#)), dynamical and statistical techniques have been developed to downscale GCMs, either producing Regional Climate Models (RCMs) with finer resolutions (10-50 km) ([IPCC, 2007](#)) or finding relationships between local and large-scale climate variables ([Fowler et al., 2007](#)).

Simulating hydrological processes associated with the transformation of rainfall into runoff in urban catchments is a widely studied topic, which provides much evidence of the application of stormwater models for assessing the impact of different rainfall events ([Knebl et al., 2005](#); [Temprano et al., 2006](#); [Barco et al., 2008](#); [Dongquan et al., 2009](#); [Qin et al., 2013](#); [Guan et al., 2015](#)). The general trend of these approaches revealed that the calibration of stormwater simulations can be enhanced and automated using statistical techniques to obtain rigorous and accurate hydrological models based on solid mathematical foundations, determined according to different goodness-of-fit measures, and consistent physical relationships related to the morphology and geometry of urban catchments. Furthermore, this previous research was developed under the stationarity assumption, whereby the mean, variance and autocorrelation of precipitation do not vary over time.

Instead, there are several studies which have focused on the projection of future values of precipitation under CC and the analysis of their impact on discharge at large catchment scales ([Dibike and Coulibaly, 2005](#); [Kleinn et al., 2005](#); [Charles et al., 2007](#); [Abdo et al., 2009](#); [Ouyang et al., 2015](#); [Pumo et al., 2016](#)). The overall tendency in these studies highlighted the lack of CC models aimed at projecting annual extreme precipitation values, which is the variable according to which urban drainage systems must be designed. Besides, most of previous methodologies were based either on the use of RCMs or the application of statistical downscaling from GCMs. Although RCMs have been proposed by several authors for developing studies at the catchment scale ([Hassan et al., 2015](#); [Kay et al., 2015](#); [Wang et al., 2015](#)), sometimes higher precision is needed, because high resolution grids (~12.5 km) are still 1,000 times larger than the common magnitude of urban catchments (few hectares). Therefore, the transition from CC models to local meteorological observations might be smoothed if both approaches are merged and statistical downscaling is applied to RCMs (“further downscaling”).

The aim of this research was therefore to design a simulation-optimization methodology to model the hydrological behavior of urban catchments through the application of Design of Experiments (DOE), in order to assess the impact of non-stationary extreme rainfall events on their response using statistical techniques to relate CC and local variables. The achievement of this objective included relevant contributions to knowledge beyond the existing literature, since they involved a DOE-based stormwater calibration procedure to

maximize the fit between simulated and observed catchment discharge based on statistically significant parameters and a simple and reliable downscaling methodology to model annual extreme rainfall events under CC scenarios using descriptive statistics. The usefulness of the proposed approach was tested through a case study of a real catchment located in Espoo, southern Finland. The trends observed in this country in relation to both urbanization and CC justified the interest in studying the hydrological response of urban catchments under non-stationary conditions in this region. A monitoring campaign recording the values of discharge at the outlet of this catchment enabled the calibration and validation of the stormwater simulations, whereas the reliability of the CC methodology was tested using three different weather stations located near the study area: Otaniemi, Nupuri and Nuuksio.

## 2. Methodology

The methodology behind this research consisted of a sequence of steps grouped into two modules as illustrated in [Figure 1](#), each of them related to the aims being sought: Module I optimized the hydrological modelling of urban catchments in terms of runoff using DOE, whilst Module II developed a descriptive statistical methodology for the projection of extreme rainfall events under CC. Hence, Module I maximized the fit between observed and simulated discharge based on identifying the most influential parameters in the response of urban catchments, in order to guarantee that their modelling under CC, which was carried out from the extreme storm events projected in Module II, was supported by solid statistical and physical relationships. The details related to each of the steps included in both modules are provided in the following subsections.

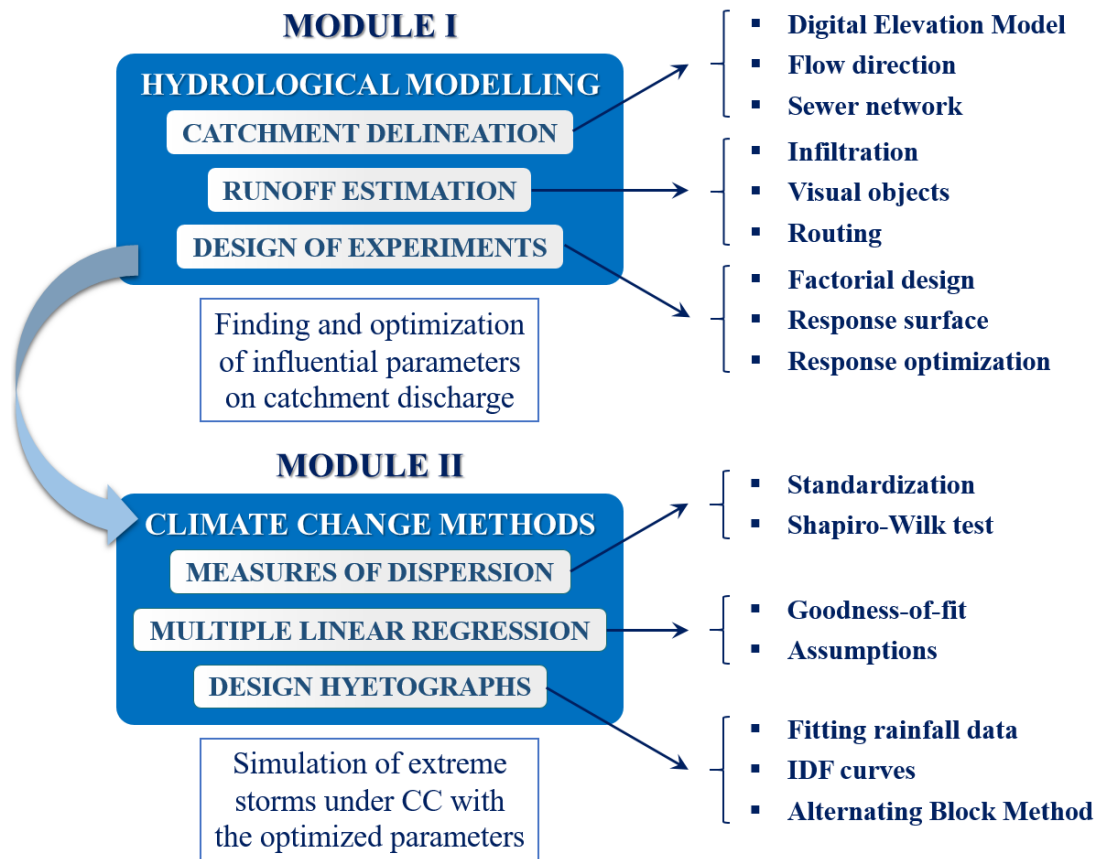


Figure 1. Outline of the two-module proposed methodology

## 2.1. Module I: Hydrological modelling of urban catchments

The first module developed a three-step methodology to optimize the hydrological modelling of urban catchments. The initial step was the delineation of the urban catchment based on three inputs: Digital Elevation Model (DEM), flow direction map and sewer network. The processing and combination of these inputs was performed using version 10.1 of [ArcGIS for Desktop \(2013\)](#). Next was the characterization and simulation of hydrological processes (infiltration and routing) and visual objects (subcatchments, manholes and pipes) through [SWMM 5.1.010 \(2015\)](#). The module concluded with the incorporation of DOE methods into the calibration procedure of the simulations run in the previous step. The desirability function approach was used to optimize the values of those parameters which were found to influence the behavior of urban catchments based on the results provided by a combination of factorial design and response surface methods. [Minitab 17 \(2014\)](#) was the statistical package chosen to carry out the analyses derived from the application of DOE.

### 2.1.1. Catchment delineation

Catchment areas were delineated from a flow direction map and stream network defined according to the cells in which flow accumulated. Flow direction was calculated using the eight direction (D8) flow model proposed by [Jenson and Domingue \(1988\)](#) from a hydro-DEM, which was determined through the smoothing of imperfections contained in the DEM, often including some cells inconsistent with neighboring pixels ([Tarboton et al., 1991](#)). In turn, the DEM was created by combining a Digital Terrain Model (DTM) and a shapefile which located buildings ([Jato-Espino et al., 2016](#)).

### 2.1.2. Runoff estimation

Runoff generated after the occurrence of a rainfall event in an urban catchment depends on the hydrological processes and entities that characterize it: infiltration, visual objects (subcatchments, manholes and pipes) and routing.

#### 2.1.2.1. Infiltration

The Soil Conservation Service (SCS) Curve Number Method ([Mockus, 1964](#)) relates runoff ( $R$ , mm) produced by a rainfall event ( $P$ , mm) to the potential maximum retention of the surface after runoff begins ( $S$ , mm) through the curve number ( $CN$ ) (see Eqs. (1) and (2)), an empirical parameter that ranges from 0 to 100 and predicts runoff production from rainfall excess. These equations assume that the relationship between initial abstraction ( $I_a$ , mm) and  $S$  is  $I_a = \lambda \cdot S$ , so that  $\lambda = 0.2$  ([Cronshey et al., 1986](#)). Although [Woodward et al. \(2003\)](#) pointed out that a value of  $\lambda = 0.05$  might be more accurate for runoff calculations, the Natural Resources Conservation Service (NRCS), formerly SCS, has made no decision on changing  $\lambda$  yet ([NRCS, 2015](#)).

$$R = \frac{(P - 0.2S)^2}{P + 0.8 \cdot S} \quad (1)$$

$$CN = \frac{25,400}{254 + S} \quad (2)$$

This method was found to be the most suitable model to characterize runoff production in urban catchments, since it can be applied using ortophotos to delineate pervious and impervious areas and determine their  $CN$  with high accuracy. The main factors that influence  $CN$  are: hydrologic soil group (HSG), cover type, hydrologic condition, antecedent runoff condition and connectivity of impervious areas to drainage systems ([Cronshey et al., 1986](#)). The solution of Eqs. (1) and (2) considering these factors and different combinations of  $S$  and  $P$  yields a series of values of  $CN$  that can be consulted in [Cronshey et al. \(1986\)](#).

### **2.1.2.2. Visual objects**

Visual objects are those required by SWMM to represent a stormwater drainage system, which includes subcatchments, conduits (pipes) and nodes (manholes). Manholes were introduced in SWMM through their elevation and depth, whilst pipes were defined using their diameter, length and roughness. SWMM applies Manning's equation to set the relationship between flow rate, cross-sectional area, hydraulic radius and slope through the pipelines. Common values for the Manning's roughness coefficient for closed conduits are given in [ASCE \(1982\)](#).

Subcatchments were defined according to nine parameters, some of which (Area, Width, Slope and % of Imperviousness) were determined using GIS-based editing and zonal statistics tools. The remaining parameters were related to the Manning's roughness coefficient and depth of depression storage of impervious and pervious areas. Typical values for these parameters can be found in [McCuen et al. \(1996\)](#) and [ASCE \(1992\)](#), respectively

### **2.1.2.3. Routing**

Flow routing through a conduit link is governed by the conservation of mass and momentum equations for both gradually varied flow and unsteady flow (i.e., the Saint Venant equations) ([Rossman, 2010](#)). From less to more complex, three different models are available in SWMM to solve these equations: steady flow, kinematic wave and dynamic wave. Since the focus of this part of the study was simulating the response of urban catchments to extreme rainfall events likely to produce flooding, the routing model was selected to keep a balance between being conservative and precise, allowing both risk management and replicating observations accurately.

Therefore, although the dynamic wave model is more correct from a theoretical point of view, the aim of the current research was to present a new stormwater simulation-optimization methodology for flood planning and not the exact replication of flow routing within the sewer system. For this reason, the kinematic wave model, which is a simplification of the dynamic wave model that ignores inertial terms in the momentum equation ([Novak et al., 2010](#)) and whose suitability for rainfall-runoff simulation at the same study catchment has been demonstrated in previous studies ([Guan et al., 2015](#)), was proposed to solve the conservation of mass and momentum equations. Besides, significant downstream flow restrictions or regulation were not expected to occur, so that the capacity of the dynamic wave model to account for back-flow effects would not make a difference.

### **2.1.3. Design of Experiments (DOE) for calibration**

Design of Experiments (DOE) analyzes the effect of input variables (factors) on an output variable (response) through a series of tests where the values of the factors are modified to check which are more influential on the response (Montgomery, 2004). A combination of two DOE types was proposed to develop calibration of the hydrological simulations carried out in SWMM: factorial and response surface designs. Factorial design was used to determine which catchment parameters were influential on discharge values, whilst a central composite design was applied to build the equations that optimized the values of such parameters in relation to the fitted response.

In addition to the linear and interaction terms contained in a factorial design equation, the relationship between the factors and the response in a surface design also includes quadratic terms (see Eq. (3)):

$$Y = \beta_0 + \sum_{i=1}^n \beta_i \cdot X_i + \sum_{i=1}^n \beta_{ii} \cdot X_i \cdot X_i + \sum_{i=1}^n \sum_{j=1}^n \beta_{ij} \cdot X_i \cdot X_j + \varepsilon \quad (3)$$

where  $Y$  is the response expressed as a non-linear combination of a set of  $n$  factors  $X_n$  multiplied by a series of coefficients  $\beta_n$  that indicate the relative weight of each term in the equation.  $\varepsilon$  represents random components (the residuals) that explain everything that cannot be interpreted from the factors.

The goodness-of-fit of these equations is traditionally calculated through a single measure such as the R-squared ( $R^2$ ) coefficient (Hirsch et al., 1993). However, Jain and Sudheer (2008) suggested that the use of a single measure for hydrological modelling can be misleading. Therefore, two additional measures were considered for testing the efficiency of the response surface equations: the Nash-Sutcliffe model efficiency coefficient ( $E$ ) (Nash and Sutcliffe, 1970) and the Root-Sum Squared Error ( $RSSE$ ).  $R^2$  is the proportion of the response variation explained by the factors in the model.  $R^2 = 1$  and  $E = 1$  refer to a perfect match of the modelled discharge to the observed data, whilst  $RSSE$  represents the deviation between observed and simulated discharges.

These measures allowed the evaluation of how well the simulations fitted the observed data for different configurations of factors. Therefore, response optimization was given by combining factors that jointly minimized  $RSSE$  and maximized  $R^2$  and  $E$ , with the limitation that the factors must remain within their lower and upper bounds. The desirability function approach was used to assess how well the combinations of factors fitted the response. Desirability ranges from 0 to 1, with 0 representing a completely undesirable value and 1 indicating an ideal response value. Derringer and Suich (1980) formulated two individual desirability functions ( $d_i$ ) depending on whether the fitted response value  $\hat{Y}_i$  must be maximised (Eq. (4)) or minimized (Eq. (5)):

$$d_i(\hat{Y}_i) = \begin{cases} 0, & \text{if } \hat{Y}_i < L_i \\ \left(\frac{\hat{Y}_i - L_i}{T_i - L_i}\right)^w, & \text{if } L_i \leq \hat{Y}_i \leq T_i \\ 1, & \text{if } \hat{Y}_i > T_i \end{cases} \quad (4)$$

$$d_i(\hat{Y}_i) = \begin{cases} 1, & \text{if } \hat{Y}_i < T_i \\ \left(\frac{\hat{Y}_i - U_i}{T_i - U_i}\right)^w, & \text{if } T_i \leq \hat{Y}_i \leq U_i \\ 0, & \text{if } \hat{Y}_i > U_i \end{cases} \quad (5)$$

where  $L_i$  and  $U_i$  are the lower and upper response values and  $T_i$  is a large enough value and a small enough value for the response when the model must be maximized and minimized, respectively.  $w$  determines how the desirability is distributed along the interval between  $L_i$  (or  $U_i$ ) and  $T_i$ . The composed desirability ( $CD$ ) of  $n$  individual desirability values  $d_i$  was calculated using the geometric mean (see Eq. (6)):

$$CD = \left( \prod_{i=1}^n d_i \right)^{1/n} \quad (6)$$

Therefore, the inclusion of DOE in the calibration of stormwater simulations maximized  $CD$ , in order to determine the configuration of catchment parameters that best fitted the monitored discharge values. The simulation-optimization of the modelling of urban catchments carried out in Module I ensured that the simulations of their response to the non-stationary storms projected in Module II were based on consistent mathematical relationships.

## 2.2. Module II: Climate Change methodology

This module built a methodology for projecting variations in extreme precipitation due to CC, in order to simulate them in SWMM according to the influential calibrated parameters identified in Module I. GCMs were considered unsuitable for CC modelling due to the huge difference in spatial resolution between their data and local observations, which facilitates the occurrence of bias in the results derived from their application. In contrast, the RCMs framed within the EURO-CORDEX initiative provide simulations with about 15 times higher resolution than GCMs. Considering that the proposed methodology was tested in Espoo (Finland), HIRHAM5 was the RCM used to project CC for being developed by the Danish Meteorological Institute, which might have a better understanding of the climate patterns in Nordic countries.

A statistics-based methodology was conceived to downscale the HIRHAM5 model to the extent of local precipitation measures, in order to model the variations in maximum rainfall due to two different Representative Concentration Pathways (RCPs) representing radiative forcing levels of 4.5 and 8.5 W/m<sup>2</sup>: RCP4.5 and RCP8.5 (Moss et al., 2008). These scenarios were modelled in relation to a stationary scenario characterized according to historical rainfall datasets, in which precipitation was assumed to remain constant over time.

Since urban drainage systems are commonly designed to deal with the greatest 24-hour rainfall amount for certain return periods, the CC methodology was developed using annual data. Therefore, the first step was the characterization of the variables contained in the HIRHAM5 model through parametric or non-parametric measures of dispersion, in order to use them as predictors to estimate the values of Annual Maximum Daily Precipitation (AMDP) for each scenario (historical or stationary, RCP4.5 and RCP8.5). The predictands to estimate through multiple linear regression were the values of AMDP recorded in several stations located near the study area. Regression models were built from the stationary scenario using real observations of AMDP to validate them according to different goodness-of-fit tests, so that they were applied to the variables included in the HIRHAM5 model for the RCPs to determine the values of AMDP under CC. Again, all statistical procedures carried out in this section were performed using Minitab 17 (2014). The last operation in Module II was the design of the synthetic hydrographs corresponding to the stationary and RCP scenarios based on the combination of Intensity-Duration-Frequency (IDF) and the Alternating Block Method.

### 2.2.1. Measures of dispersion

Since the predictand was a yearly measured value such as AMDP, the variables included in the HIRHAM5 model to perform as predictors were represented using annual data too. Hence, two standardized measures of dispersion ( $MD$ ) were proposed to characterize them depending on whether their annual datasets were normally distributed or not: coefficient of variation ( $CV$ ) and interquartile ratio ( $IR$ ) (see Eq. (7)):

$$MD = \begin{cases} CV = \frac{\sigma}{\bar{x}}, & \text{if the dataset is normally distributed} \\ IR = \frac{IQR}{\tilde{x}}, & \text{if the dataset is not normally distributed} \end{cases} \quad (7)$$

where  $\bar{x}$  is the mean,  $\tilde{x}$  is the median,  $\sigma$  is the standard deviation and  $IQR$  is the interquartile range of the dataset. These measures of dispersion are useful to capture the overall distribution of a variable throughout a year, since they include information on both its

spread and central values. This representativeness enabled their use as predictors to set correlations with other summary statistics such as the maximum annual value of a sample (AMDP).

The choice between *CV* and *IR* was approached using normality tests. The Shapiro-Wilk test, which has been found to be more reliable when checking normality than Kolmogorov-Smirnov or Lilliefors tests (Shapiro et al., 1968), was selected for checking normality. A value of  $\alpha$  equal to 0.05 was chosen for statistical testing, indicating whether *CV* ( $\alpha > 0.05$ ) or *IR* ( $\alpha < 0.05$ ) had to be chosen for characterizing the predictors required to estimate AMDP.

### 2.2.2. Multiple linear regression

The concept of regression was already introduced in a polynomial form in Eq. (3). Multiple linear regression is simpler, since it models the relationship between two or more explanatory predictors and a response through a linear equation (see Eq. (8)). In the context of Module II, multiple linear regression was used to create equations for the estimation of AMDP from a series of CC variables included in the HIRHAM5 model.

$$Y = \beta_0 + \beta_1 \cdot X_1 + \beta_2 \cdot X_2 + \dots + \beta_k \cdot X_k + \varepsilon \quad (8)$$

where  $Y$  is the predictand expressed as a linear combination of  $k$  predictors  $X_k$  which are multiplied by weights  $\beta_k$  that indicate their importance in the model. The equation also includes a constant  $\beta_0$  and the residuals  $\varepsilon$ , which complete the information provided by the independent variables.

The standard  $R^2$  has several limitations that compromise its validity to measure the goodness-of-fit of regression models for making new estimates. Although the adjusted  $R^2$ , which emerged as a modified version of the standard  $R^2$ , improves its reliability by capturing the influence of the number of predictors on the fitting of the model, its ability to provide accurate predictions of new data is still limited. Hence, the predicted  $R^2$  and the standard error of the regression ( $S$ ), whose combination overcomes this drawback and can make reliable predictions for new observations, were used for assessing the goodness-of-fit of regression models.

Cook's distance ( $s_i$ ) was used to show the influence of each observation  $i$  on the predictand and identify outliers in the regression models. According to Eq. (9), an observation with a value of  $s_i$  larger than three times the mean Cook's distance of the whole dataset is considered an outlier (Stevens, 2009):

$$s_i = \frac{\sum_{j=1}^n (y_j - \hat{y}_j)^2}{(k + 1) \cdot MSE} \quad (9)$$

where  $MSE$  is the mean squared error of the regression model,  $y_j$  is the  $j$ th fitted predictand value and  $\hat{y}_j$  is the  $j$ th fitted predictand value where the fit omits observation  $i$ .

Multiple linear regression is based on four assumptions that must be verified to ensure its validity. These assumptions are related to the analysis of the residuals of the regression models and can be divided into four (Tabachnick and Fidell, 1989): linearity, independence, homoscedasticity and normality. Violation to these assumptions was diagnosed through the p-value of the Analysis of Variance (ANOVA) (Fisher, 1925), the Durbin Watson statistic (Durbin and Watson, 1950; Durbin and Watson, 1951) and the Levene's (Levene, 1960) and Shapiro-Wilk tests, respectively.

### 2.2.3. Design hyetographs

Design hyetographs, which are representations of the distribution of rainfall over time, were determined to simulate the hydrological response of urban catchments after the occurrence of extreme storms caused by CC. They were created using the Alternating Block Method from IDF curves calculated for different values of fitted annual precipitation.

#### 2.2.3.1. Fitting of probability distributions to rainfall data

Rainfall data consisted of a set of daily precipitation measures arranged according to unknown distribution patterns which were processed to obtain the values of AMDP associated with the return periods used to design the hyetographs with which to test the response of urban catchments under the stationary and RCP scenarios. The Anderson-Darling test (Anderson and Darling, 1954), which has been proved to be more powerful than the Kolmogorov-Smirnov test for this purpose (Shapiro et al., 1968), was used to find the probability distribution that best fitted patterns of precipitation. This test considers the specific distributions being tested in the calculation of its critical values, which increases the sensitivity of results (Stephens, 1974).

#### 2.2.3.2. Intensity-Duration-Frequency (IDF) curves

IDF curves were built using representative points of the average intensity of precipitation for different durations corresponding to the same frequency of return period (Témez, 1978). The modelling of IDF curves began by relating the values of AMDP obtained in the previous step for different return periods according to the Anderson-Darling statistic to a series of rainfall durations ( $D$ ) less than or equal to 24 hours through the coefficients

of relationship ( $R$ ) proposed by Campos Aranda (1998) in Table 1, which enabled determining values of maximum precipitation ( $P$ ) per duration. These values are conservative and therefore result in storms that lead to be in the safe side in terms of design, which is consistent with the strategy followed for the routing model.

**Table 1.** Coefficients of relationship to determine precipitation for different rainfall durations

$D$ (h)	1	2	3	4	5	6	8	12	18	24
$R$	0.30	0.39	0.46	0.52	0.57	0.61	0.68	0.80	0.91	1.00

The intensity  $I$  was calculated as the ratio between each pair of values of  $P$  and  $D$ . The approach proposed by Aparicio (1997) (see Eq. (10)) was chosen for the analytical representation of the IDF curves, because of its relationship to the statistical methods already used in the methodology.

$$I = \frac{K \cdot T^m}{D^n} \quad (10)$$

where  $I$ ,  $T$  and  $D$  are expressed in mm/h, years and hours, respectively, and  $K$ ,  $m$  and  $n$  are parameters to estimate through multiple linear regression analysis (see Eq. (11)). Thus, the terms shown in Eq. (8) are replaced according to Eq. (10) as follows:

$$\log I = \log K + m \cdot \log T - n \cdot \log D + \varepsilon \quad (11)$$

such that  $\log I = Y$ ,  $\log T = X_1$ ,  $\log D = X_2$ ,  $\log K = \beta_0$ ,  $m = \beta_1$  and  $n = \beta_2$  in relation to Eq. (8). Hence, the values of the parameters that characterize the IDF curves were determined from the regression coefficients.

### 2.2.3.3. Alternating Block Method

The Alternating Block Method (Chow et al., 1988) was used for designing synthetic storms from IDF curves according to  $n$  time intervals  $\Delta t$ , such that the total duration  $D$  of the storm event is equal to  $n \cdot \Delta t$ .  $D$  was assumed to be the lag time of the longest flow path in the catchment.

For a given return period, the procedure consisted of the determination of the intensity for the durations  $\Delta t$ ,  $2\Delta t$ , ...,  $n\Delta t$  using Eq. (10) to obtain total precipitation by multiplying intensities by durations (Gómez Valentín, 2007). Once the process was applied to every interval into which the storm duration was divided, the values of precipitation were arranged in descending order alternately to the right and left of the central block to form the design hyetograph.

### 3. Results and discussion: a case study in Espoo, Finland

The results were obtained by applying the methodology to a real catchment located in Espoo, southern Finland. Figure 2a) shows the location of the study catchment and the geometrical arrangement of its sewer network. The study catchment rapidly evolved from a coniferous forest in 2001 to a residential area in 2006, when the construction of the sewer network and buildings finished (Sillanpää, 2013; Guan et al., 2015; Sillanpää and Koivusalo, 2015). The geometrical arrangement of the sewer network and the permission to use it were provided by the Helsinki Region Environmental Services Authority HSY.

Figure 2a) also includes the orthophoto of the catchment area when a degree of fully development in late 2006 was reached, obtained via WMS (Web Map Service) through the Map Service of Espoo ( espoo.fi, 2016). A Digital Terrain Model (DTM) was acquired from the National Land Survey of Finland in ASCII format with a cell size of 2 m (NLS, 2016). Information from the Geological Survey of Finland revealed that the study catchment was covered by a layer of sandy till with bedrock below it (Guan et al., 2015), which corresponds to a HSG of A or at least B (Cronshey et al., 1986).

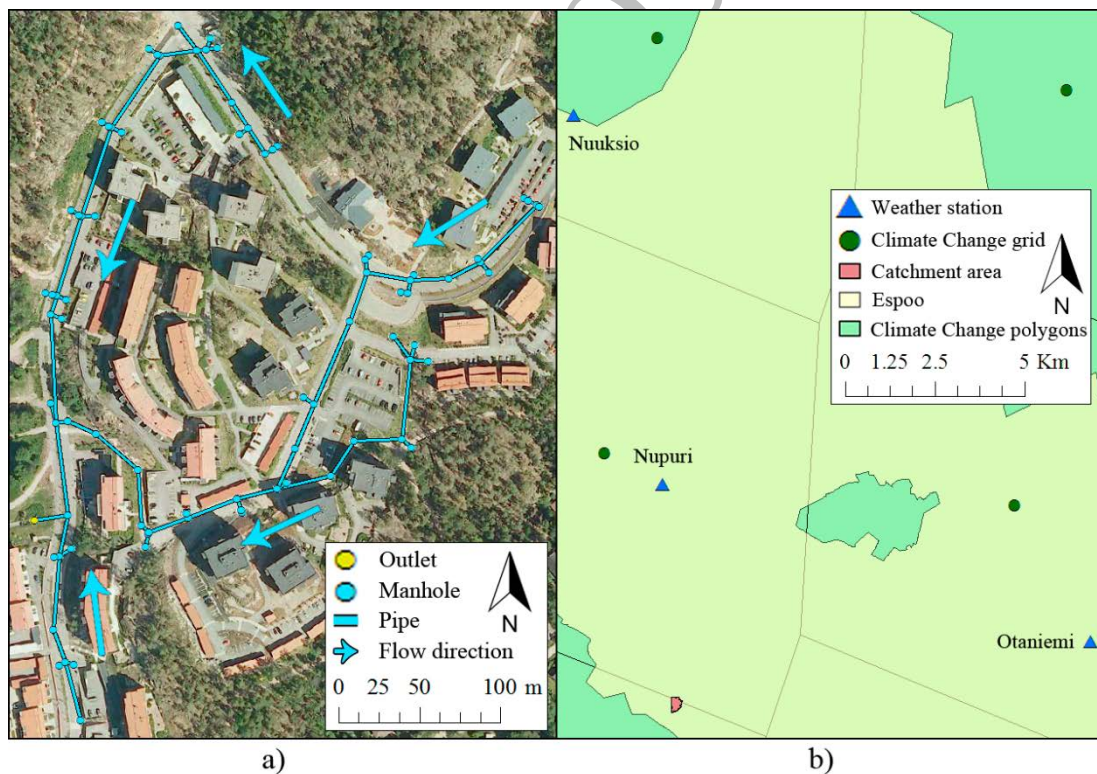


**Figure 2.** a) Location of the study catchment and its drainage network b) Spatial arrangement of the datasets required to develop the Climate Change model

The remaining datasets required to apply the methods included in Module I were the values of precipitation and flow in the outlet of the catchment, which were monitored during

2006 (Sillanpää, 2013). Precipitation was recorded every 2 minutes using a weather station with an ARG100 tipping bucket rain gauge, which enabled reaching a volume resolution of 0.2 mm. Water depth was monitored at a v-notch weir located at the catchment outlet with the same temporal resolution than precipitation, so that flow rates were calculated using a stage-discharge curve for the weir based on the amount of water measured. Table 2 summarizes the main characteristics of the set of rainfall-runoff events chosen for calibration and validation, which were selected to have a representative sample of durations and intensities.

**Table 2.** Summary of the rainfall events used for simulation

Event	Duration (h)	Depth (mm)
CAL 1	5:52	5.0
CAL 2	11:26	37.4
CAL 3	6:58	12.2
VAL 1	6:36	5.2
VAL 2	4:48	9.0
VAL 3	6:48	23.4

Regarding Module II, Figure 2b) provides a scheme of the spatial arrangement of the grid with the 56 CC variables included in the HIRHAM5 model, as well as the location of the three weather stations with historical rainfall data and the study catchment. The polygons in Figure 2b), which stand for the influential areas associated with each point in the HIRHAM5 grid, were drawn to relate each weather station to its nearest CC point. Hence, the regression models built for each station were calculated from the CC datasets corresponding to their closest points in the grid. These datasets covered periods of 55 (1951-2005) and 95 (2006-2100) years for the stationary and RCP scenarios, respectively. In accordance with the upper limit of the stationary scenario (2005), the historical rainfall daily datasets available for the weather stations in Otaniemi, Nupuri and Nuuksio consisted of 55, 45 and 40 years (Klein Tank et al., 2002).

### 3.1. Module I: Hydrological modelling of urban catchments

The datasets with georeferenced information on the DTM, buildings and sewer network were used to delineate the study catchment. Figure 3a) represents the DEM produced after merging the original DTM and the vector layer of buildings in the area, as well as the subcatchments obtained through the combination of the sewer network with the flow direction map. The whole catchment covered a total area of 10.535 ha, including 79 subcatchments with an average area of 0.133 ha. Both percentage of imperviousness and *CN* were calculated from the orthophoto of the study area, which was used to delineate pervious and impervious areas within the catchment and, by extension, identify the cover types and hydrologic condition that defined their *CN* (see Figure 3b)). The application of zonal

statistics based on the relationship between these values and the area of the subcatchments yielded the inputs required for parameterizing these visual objects in SWMM.

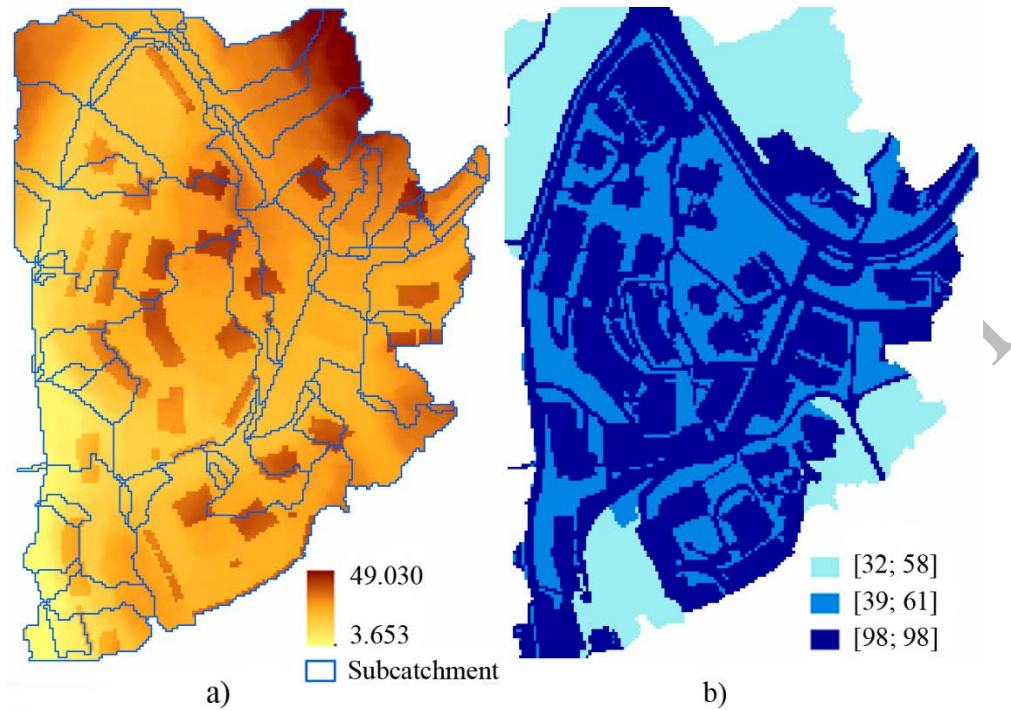


**Figure 3.** a) Digital Elevation Model (m) and catchment delineation b) *CN* values in the catchment area

The number of stormwater simulation runs was determined using DOE. The set of 9 parameters or factors introduced in SWMM were: percentage of imperviousness ( $a$ , %), width ( $b$ , m), slope ( $c$ , %), Manning's roughness for impervious area ( $d$ ), depth of depression storage on impervious area ( $e$ , mm), Manning's roughness for conduits ( $f$ ), Manning's roughness for pervious area ( $g$ ), depth of depression storage on pervious area ( $h$ , mm) and curve number ( $i$ ). Since the number of factors was high, a factorial design was used as an exploratory analysis to identify which parameters had a statistically significant influence in the results of the simulations.

The experiment consisted of a  $1/4$  fractional design at 2 levels, reaching the highest possible resolution for this combination of levels and factors. The design was developed for the first calibration event (CAL 1) exclusively (see [Table 2](#)), because its aim was not the calibration of the simulations itself but only the determination of significant predictors. Although the intensity of the effect of the predictors on the predictand might vary depending on the characteristics of the event, the presence of interactions was assumed to be constant. All factors were introduced as continuous variables, except  $i$ , which was incorporated into the design as a dichotomous variable, such that 0 and 1 related to HSGs equal to A and B, respectively. Factors from  $d$  to  $h$  were defined according to their lower and upper bounds according to values found in specialized literature ([McCuen et al.](#),

1996); ASCE, 1992), whereas factors  $a$ ,  $b$  and  $c$  represented the error in GIS-based parameters, so that deviations up to 20% in both directions set their limits.

The combination of these factors resulted in 130 runs which demonstrated that variations in three of them ( $g$ ,  $h$  and  $i$ ) did not have a statistically significant impact on the simulations, which was consistent with the results obtained by Krebs et al. (2013) in Finnish urban catchments. Influential factors were identified according to the p-value of the terms in the regression models obtained for the three goodness-of-fit measures considered:  $R^2$ ,  $E$  and  $RSSE$ . Since the p-values of factors  $g$ ,  $h$  or  $i$  were above 0.05, they were discarded for further calculations. The most influential predictors were found to be those related to the imperviousness of the catchment area ( $a$  and  $e$ ), contributing more than 70% to estimate  $R^2$ ,  $E$  and  $RSSE$ . Moreover, the excellent values of predictive  $R^2$  (0.997, 0.999 and 0.980) reached for the three goodness-of-fit measures supported the assumption that the significance of the interactions between the predictors and the responses could be extrapolated to other rainfall events.

The information inferred from the factorial design enabled characterizing the central composite design for calibrating the simulations. This experiment consisted of a 6-factor  $1/2$  central composite design, which resulted in 45 runs that were simulated for three calibration events: CAL 1, CAL 2 and CAL 3 (see Table 2). Figure 4 represents the results obtained for these events through boxplots according to the values of  $R^2$ ,  $E$  and  $RSSE$  reached, proving the importance of using more than one goodness-of-fit measure for hydrological modelling.  $R^2$ , which is the most widely used coefficient for this purpose, was found to yield especially misleading values for CAL 2 and CAL 3. In contrast,  $E$  demonstrated to be very sensitive to the variations in the parameters involved by the different runs designed.

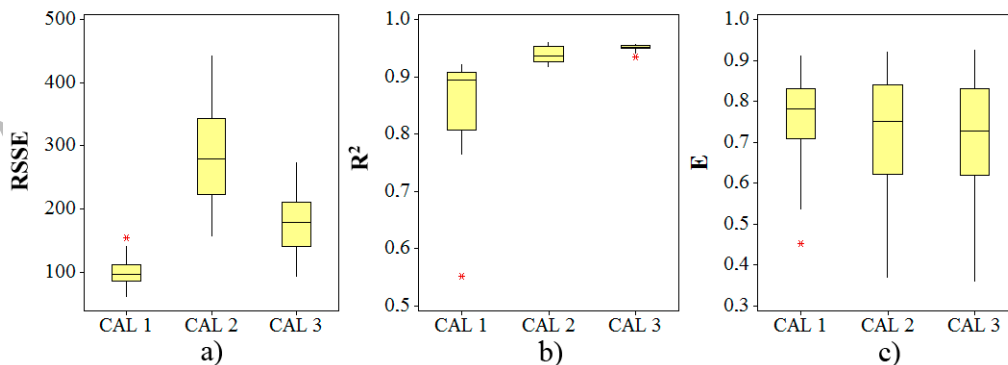


**Figure 4.** Boxplots with the 45 values of a)  $RSSE$  b)  $R^2$  c)  $E$  obtained for the three calibration events

The values depicted in Figure 4 were used to build multiple linear regression models for the events CAL 1, CAL 2 and CAL 3 as shown in Table 3, confirming that  $a$  and  $e$  were the main contributing factors to the calibration of the simulations run in SWMM. CAL 1

was the event that resulted in the lowest  $S$  values (7.792, 0.014 and 0.034), which validated its selection as a representative and demanding event for the factorial design. In general, all coefficients of determination were close to 1, which guaranteed that the 6 factors selected from the factorial design enabled an accurate modelling of the hydrological response of the study catchment. The only exception to this trend was found in the values reached for  $R^2$  in the event CAL 3, which barely reached coefficients of determination of 0.5, due to its little sensitivity to the variations in the factors (see Figure 4b)). This circumstance highlighted the importance of considering the standard error of the regression as an alternative measure of the quality of regression models, because  $S$  precisely reached its best value (0.003) for  $R^2$  in this calibration event.

**Table 3.** Multiple linear regression models obtained with the 6-factor 1/2 central composite design

Event	Goodness-of fit measure	$S$	$R^2$	Adj. $R^2$	Pred. $R^2$
CAL 1	$RSSE$	7.792	0.878	0.859	0.766
	$R^2$	0.014	0.965	0.960	0.915
	$E$	0.034	0.909	0.895	0.830
CAL 2	$RSSE$	3.818	0.997	0.996	0.993
	$R^2$	0.004	0.932	0.925	0.771
	$E$	0.005	0.998	0.998	0.997
CAL 3	$RSSE$	1.636	0.999	0.998	0.997
	$R^2$	0.003	0.554	0.509	0.409
	$E$	0.005	0.999	0.999	0.997

The information compiled in Table 3 was used to determine the desirability functions for maximizing  $R^2$  and  $E$  and minimizing  $RSSE$  through the application of Eqs. (4) and (5). Table 4 shows the calibrated values for the six significant parameters, as well as the initial values with which the optimization process was started, which coincided with the mean of the ranges considered. Similar previous studies (Guan et al., 2015) did not considered percentage of imperviousness ( $a$ ) for calibration; however, the use of DOE proved that this parameter had a major impact on the simulations. Moreover, its calibrated value (see Table 4) was consistent with the results achieved by Sillanpää (2013), who concluded that the effective impervious fraction for the study catchment was about 74% of its total impervious area.

Despite the individual variations in the factors included in Table 4, the combined effect of the calibration enabled their balance. Hence, both percentage of imperviousness ( $a$ ) and depth of depression storage on impervious area ( $e$ ) were reduced in relation to their initial values, so that the increase in pervious area ( $a$ ) was compensated by the decrease of volume to be filled prior the occurrence of runoff ( $e$ ). Similarly, a decrease in width ( $b$ ) resulted in longer flow paths, whereas steeper slope ( $c$ ) produced an increase in the

velocity at which water was conveyed. The Manning's roughness coefficient for impervious area ( $d$ ) did not vary in relation to its initial value,

**Table 4.** Calibration of the six parameters that had significant interactions with the response variable

Term	Factor	Min	Max	Initial value	Calibrated value
$a$	Percentage of imperviousness	0.800	1.200	1.000	0.800
$b$	Width	0.800	1.200	1.000	0.804
$c$	Slope	0.800	1.200	1.000	1.151
$d$	Manning's roughness for impervious area	0.011	0.016	0.014	0.014
$e$	Depth of depression storage on impervious areas	0.000	2.500	1.250	0.379
$f$	Manning's roughness for conduits	0.011	0.015	0.013	0.015

The integration of the individual desirability values obtained from the three calibration events using the parameters shown in Table 4 through Eq. (6) yielded the results shown in Table 5. The value of  $CD$ , which was almost 1, indicated that the use of these calibrated values provided a very accurate modelling of the real hydrological response of the study catchment. The interpretation of these values in terms of the results obtained for the runs in the central composite design (see Figure 4) suggested a slight overfit in some of the goodness-of-fit measures, due to the errors in the regression models.

**Table 5.** Composed desirability and values of  $R^2$ ,  $E$  and  $RSSE$  achieved using DOE

$C.D.$	CAL 1			CAL 2			CAL 3		
	$RSSE$	$R^2$	$E$	$RSSE$	$R^2$	$E$	$RSSE$	$R^2$	$E$
0.996	62.115	0.919	0.911	118.830	0.959	0.946	90.172	0.957	0.938

The validation events VAL 1, VAL 2 and VAL 3 (see Table 2) were simulated using the calibrated parameters compiled in Table 4, in order to ensure their reliability. Figure 5 depicts the hydrographs corresponding to the application of these values to both the calibration and validation events. The mere visual inspection of these plots demonstrated the accuracy of the proposed DOE-based methodology for calibrating urban catchments. Moreover, the comparison between the values of  $R^2$ ,  $E$  and  $RSSE$  obtained for the calibration events (see Table 6) and those represented by the boxplots in Figure 4 proved the optimality of the results. The differences between the values shown in Table 5 and Table 6 confirmed the overfit in the results obtained using the desirability function approach, which resulted in more conservative hydrographs (slight overestimation of the volume of water accumulated). Furthermore, the validation events reached even higher values in the goodness-of-fit measures than the calibration events, which demonstrated the validity of the results for modelling new events.

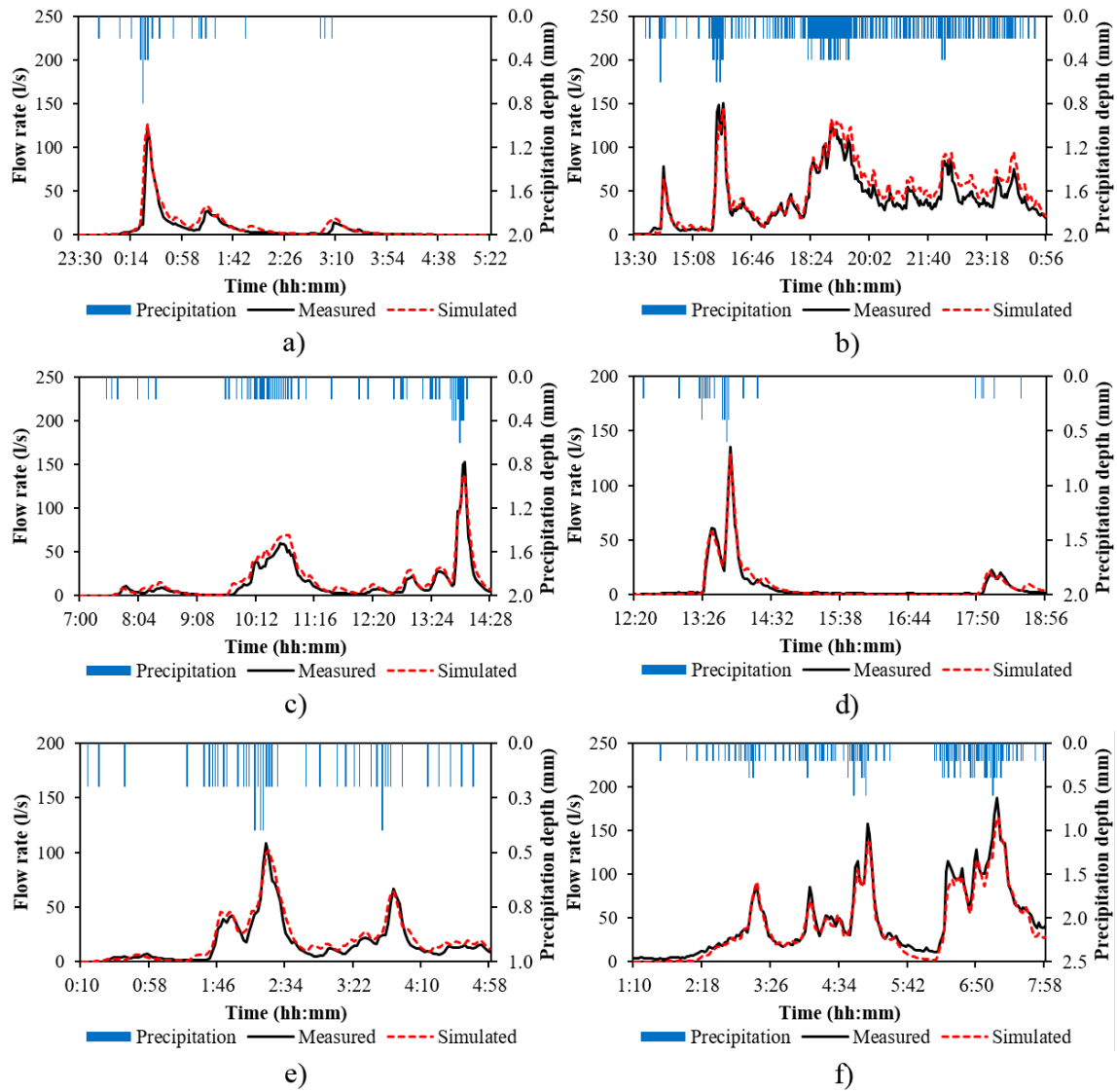


**Figure 5.** Fitting between observed and predicted hydrographs for the calibration and validation events a) CAL 1 b) CAL 2 c) CAL 3 d) VAL 1 e) VAL 2 f) VAL 3

**Table 6.** Values of  $RSSE$ ,  $R^2$  and  $E$  obtained for the calibration and validation events using DOE

Event	$RSSE$	$R^2$	$E$
CAL 1	81.937	0.905	0.845
CAL 2	212.805	0.928	0.855
CAL 3	92.666	0.959	0.927
VAL 1	42.465	0.973	0.973
VAL 2	68.256	0.952	0.921
VAL 3	115.639	0.974	0.960

### 3.2. Module II: Climate Change methodology

Normality of the CC variables contained in the HIRHAM5 model was checked for each year in the closest grid points to the weather stations (see Figure 2b)) using the Shapiro-

Wilk test, in order to determine whether *CV* or *IR* was the most suitable measure of dispersion to characterize them using Eq. (7). The results proved that only 13% of the variables followed normal distributions for the years and meteorological stations considered. Error checking in the daily rainfall datasets of Otaniemi, Nupuri and Nuuksio demonstrated that these stations contained 55, 42 and 39 valid years for modelling, respectively. Values of AMDP were calculated for these valid years to determine the predictands with which to build the regression models. Table 7 summarizes the main characteristics of the models built for the three stations. Again, these regression models were built stepwise to select those predictors that were statistically significant at the 95% confidence level ( $p$ -value  $< 0.05$ ). The calculation of the Cook's distance (see Eq. (9)) highlighted some outliers in all three cases, which were discarded to avoid bias and unrepresentativeness. However, the regression models shown in Table 7 were still valid for 47, 36 and 33 points, which means more than 85% of the initial sample for the three stations.

The results included 19, 17 and 18 of the 56 variables available in the HIRHAM5 model for estimating AMDP in Otaniemi, Nupuri and Nuuksio, respectively, so that the relationships between predictors and predictand were supported by physical foundations. Precipitation stands for any product of atmospheric water vapor (*prw*) (Glickman, 2000) that falls due to gravity from clouds (*clt*) and consists of water and ice crystals (*clvi*, *clwvi*) (Matveev and Matveev, 2009). The formation of clouds from which precipitation falls is preceded by the processes of evaporation (*evspsbl*) and transpiration, which contribute to increase the amount of water in the air and the cooling of air to the dew point due to its rise (*zg200*) (Menzhulin, 2009). The incident solar radiation on Earth (*rhus*, *rlut*, *rsds*, *rsdt*, *rsut*) heats its surface (*hfls*, *sund*, *tasmax*) and air, which enables the rise (*ta200*, *ta500*, *ta850*), expansion and cooling of this warm air (Chapin et al., 2011). Wind (*sfcWind*, *sfcWindmax*, *uas*, *vas*) in low pressure areas (*ps*) is another phenomenon that forces air to rise (*ua850*, *va500*, *va850*) and create turbulences in the air (Ahrens and Samson, 2011a). Mountains and similar landforms that make topography slopes upwards can also induce wind stress (*tauu*, *tauv*) (Schwab and Beletsky, 2003). Warm and cold weather fronts, which usually delimit the threshold from which air differs in temperature and humidity (*huss*), have an impact on the formation of clouds too, because they lead to situations in which warm air rises above cold air and cold air moves warm air up (*hus850*), respectively (Ahrens and Samson, 2011b). Finally, the links between the predictand and the infiltration (*mrro*, *mrso*) and precipitation-related CC variables (*pr*, *prc*, *prhmax*) are given by causal relationships, since surface moisture depends on the amount of rainfall and different types of precipitation are all related to each other.

**Table 7.** Multiple linear regression models to predict AMDP in the three weather stations

Term	Otaniemi		Nupuri		Nuukio	
	Coef	p-value	Coef	p-value	Coef	p-value
Regression	-	0.000	-	0.000	-	0.000
Constant	-45.50	0.007	-1866.00	0.000	-76.50	0.000
Column Ice Water Content (clivi)	10.44	0.000	-14.14	0.000	-	-
Total Cloud Cover clt	-17.49	0.000	-	-	30.20	0.000
Column Condensed Water Content (clwvi)	-10.42	0.000	-	-	-17.34	0.000
Surface Evaporation (evspsbl)	-	-	-	-	-341.70	0.000
Surface Latent Heat Flux (hfls)	-	-	-	-	385.30	0.000
Specific Humidity at 850 hPa (hus850)	49.92	0.000	-	-	-	-
Near-Surface* Specific Humidity (huss)	-61.50	0.000	-61.04	0.000	66.51	0.000
Total Runoff (mrro)	1.92	0.000	0.76	0.000	-1.78	0.000
Total Soil Moisture Content (mrso)	-	-	-119.10	0.000	-59.46	0.000
Precipitation (pr)	-	-	3.96	0.000	-	-
Convective Precipitation (prc)	-1.28	0.000	-5.02	0.000	-	-
Daily-Max. 1-hour Precipitation Rate (prhmax)	-	-	2.89	0.001	-	-
Column Water Vapor (prw)	-	-	-	-	-24.06	0.000
Surface Pressure (ps)	-	-	-971.00	0.005	-	-
Upwelling Longwave radiation (rlus)	177.20	0.000	-	-	-	-
TOA Outgoing Longwave Radiation (rlut)	179.00	0.000	-	-	215.90	0.000
Surface Downwelling Shortwave Radiation (rsds)	-	-	-	-	16.62	0.000
TOA Incident Shortwave Radiation (rsdt)	-	-	1217.00	0.000	-	-
TOA Outgoing Shortwave Radiation (rsut)	13.55	0.049	-	-	-10.05	0.010
Near-Surface* Wind Speed (sfcWind)	-110.73	0.000	-	-	17.46	0.010
Daily-Max. Near-Surface* Wind Speed (sfcWindmax)	-	-	-	-	-843.00	0.000
Sunshine Hours (sund)	11.32	0.000	29.37	0.000	-	-
Temperature at 200 hPa (ta200)	1132.00	0.000	690.20	0.000	662.10	0.000
Temperature at 500 hPa (ta500)	1277.00	0.000	1049.00	0.000	-	-
Temperature at 850 hPa (ta850)	-1464.00	0.000	-1099.00	0.000	-	-
Daily-Max. Near-Surface* Air Temperature (tasmax)	-	-	1745.00	0.000	-	-
Surface Downward Eastward Wind Stress (tauu)	-	-	-0.21	0.000	0.18	0.000
Surface Downward Northward Wind Stress (tauv)	-0.47	0.000	-	-	-	-
Zonal (Eastward) Wind at 850 hPa (ua850)	-	-	-	-	5.41	0.000
Eastward Near-Surface* Wind (uas)	-0.02	0.000	-	-	-	-
Meridional (Northward) Wind at 500 hPa (va500)	-0.06	0.000	-	-	-	-
Meridional (Northward) Wind at 850 hPa (va850)	-	-	-	-	-0.07	0.000
Northward Near-Surface* Wind (vas)	0.39	0.000	-0.09	0.000	-	-
Geopotential Height at 200 hPa (zg200)	-	-	433.00	0.011	-1005.80	0.000
<b>S</b>		2.552		2.592		1.168
<b>R<sup>2</sup></b>		0.957		0.975		0.993
<b>Adj. R<sup>2</sup></b>		0.927		0.952		0.983
<b>Pred. R<sup>2</sup></b>		0.792		0.892		0.942

\* Near-Surface means at a height between 1.5 to 10.0 m.

The standard  $R^2$  coefficients included in Table 7 indicated that 95.7%, 97.5% and 99.3% of the variation of AMDP was explained by the variables extracted from the HIRHAM5 model. The adjusted  $R^2$  values proved that the number of predictors chosen was adequate in each case, which ensured that the models were not overfitted. In fact, the homogeneity in the Variance Inflation Factor (VIF) obtained for the predictors, which was always below 6, ensured that they were not highly correlated to each other and multicollinearity was not an issue. Furthermore, the high and low values of predicted  $R^2$  and  $S$  guaranteed the reliability of the regression models for making new estimates and therefore validated them to predict the values of AMDP associated with the RCP scenarios.

The p-value of the regression models, which was always below the significance level (see Table 7), confirmed the linearity of residuals. Furthermore, the values reached regarding the Shapiro-Wilk and Levene's statistics enabled accepting the null hypotheses in all cases (p-values > 0.05), which involved that the residuals were normally distributed and had homogeneous variances. The Durbin-Watson statistic was found to be inconclusive for evaluating the independence of residuals, since the values reached for all three cases were within their lower and upper critical values. Therefore, this assumption was exclusively checked through the visual inspection provided by the standardized residuals versus order plots depicted in Figure 6. The absence of time trends and positive and negative serial correlations provided more than enough evidence of the independence of residuals.

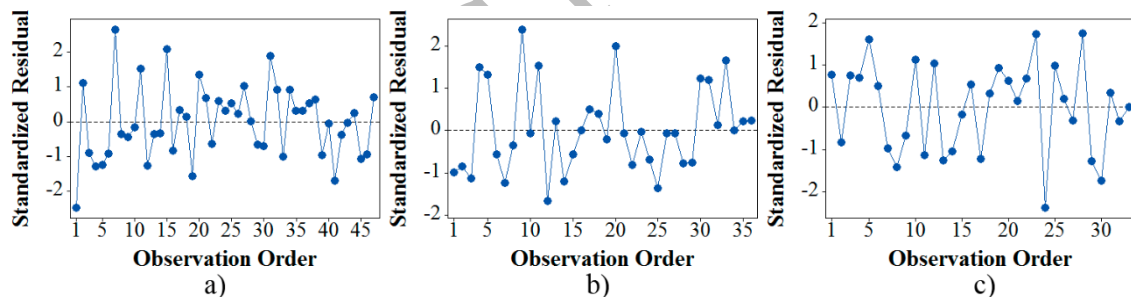


**Figure 6.** Standardized residuals versus order of data for the three stations a) Otaniemi b) Nupuri c) Nuukisio

Since Nupuri was the closest meteorological station to both the study catchment and the HIRHAM5 grid (see Figure 2b)) and recorded the most extreme rainfall measures, subsequent calculations were particularized to its regression model. The period of analysis selected for the RCP scenarios was 2059-2100 (42 years), in order to replicate the same initial conditions under which the regression model for Nupuri was built and represent the worst situation in terms of greenhouse gas concentration, since the RCPs simulations of the HIRHAM5 model cover the period from 2006 to 2100. As in the stationary scenario, the general trend for the RCP scenarios indicated that  $IR$  was the adequate measure of dispersion to model most of the predictors (p-values < 0.05). In this case, about 18% of the variables were normally distributed for the years considered in the modelling of

RCPs. Based on this information, the set of 17 predictors for Nupuri (see Table 7) were characterized using Eq. (7), which resulted in the time series shown in Figure 7 for both the stationary and RCP scenarios. Figure 7a) exhibits the great capability of the model to fit a variety of values of AMDP, including pronounced peaks and sinks. In overall terms, the excellent results provided by the three models certified the suitability of the proposed methodology to predict extreme precipitation and the usefulness of the two measures of dispersion to capture the overall behavior of CC variables and set relationships to the real values of AMDP measured in the stations. The time series for the RCPs depicted in Figure 7b) excludes the six values that were farthest from the median in both datasets (not necessarily outliers), in order to include the same final number of points (36) for which the regression model associated with Nupuri was valid.

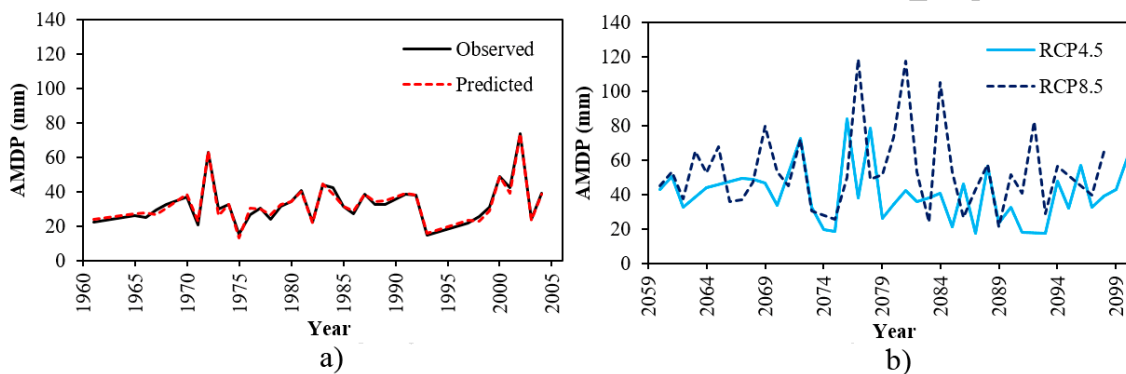


**Figure 7.** Annual Maximum Daily Precipitation (AMDP) time series in the weather station in Nupuri a) Stationary b) RCPs

The values in these time series were used to find the probability distributions that best fitted them and obtain the values of AMDP listed in Table 8. According to the Anderson-Darling statistic, the Burr distribution (Shao et al., 2004) and the Wakeby function (Houghton, 1978) provided the best fit for the stationary and RCP scenarios, respectively. The almost perfect match between observed and predicted stationary values of AMDP, especially for short return periods, confirmed the validity of the proposed regression-based methodology for projecting CC. The RCPs involved increases of 20-30% and 60-80% in AMDP in comparison with the stationary values, which supported the interest in studying the effects of CC on the hydrological response of urban catchments.

**Table 8.** Values of AMDP (mm) fitted with the Burr and Wakeby distributions for the scenarios and return periods (T) under consideration

Return Period	Stat. Obs.	Stat. Pred.	RCP4.5	RCP8.5
	Burr	Burr	Wakeby	Wakeby
2	31.161	31.260	38.987	49.628
5	40.207	40.011	51.441	68.599
10	46.819	46.357	60.188	84.044
25	56.412	55.506	73.283	106.22
50	64.674	63.339	84.656	124.420
100	74.033	72.170	97.483	143.970

IDF curves were determined from these values of AMDP through Eqs. (10) and (11), resulting in predicted  $R^2$  coefficients of 0.998, 0.998, 0.997 and 0.993 for Stat. Obs., Stat. Pred., RCP4.5 and RCP8.5, respectively. Since the predictors  $D$  and  $T$  consisted of 10 and 6 values (see Table 1 and Table 8) repeated and combined for each value of  $I$ , the information contained in the residuals was meaningless, because all the assumptions were distorted due to the stepped arrangement of the individual points used to build the models. Therefore, these results were accepted as valid based on the almost perfect fit indicated by the predicted  $R^2$ .

The duration of the study catchment, calculated as the longest sewer travel time, resulted in 106 minutes, which was consistent with the trend of the rainfall events monitored in 2006. Its division into several intervals and the application of the Alternating Block Method provided the hyetographs required to model the climatological conditions that defined the stationary and RCP scenarios. Their representation, as well as those of the hydrographs obtained from their simulation in SWMM using the calibrated parameters listed in Table 4, is given in Figure 8.

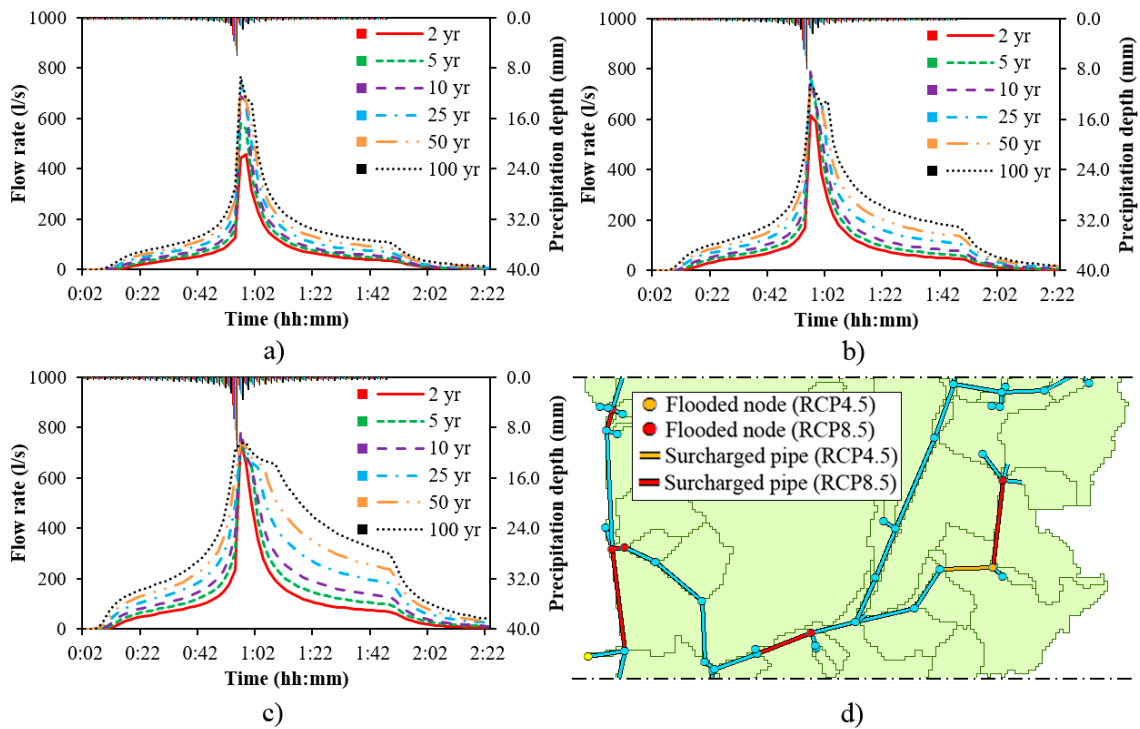


**Figure 8.** Design hydrographs for the return periods and scenarios under analysis a) Stat. b) RCP4.5 c) RCP8.5 d) Flooded nodes and surcharged pipes for a return period of 2 years under the RCPs

The peaks and overall volumes associated with the RCP hydrographs indicated the great increase in drainage requirements involved by CC. The simulations proved that the RCP hydrographs for a return period of 2 years were enough to produce floods and surcharges in some nodes and conduits of the sewer network (see Figure 8d)). In fact, the peak flows obtained for the RCP8.5 scenario were almost identical for all the return periods in the range between 2 and 100 years. This situation was associated with the most extreme rainfall conditions, which favored the occurrence of node flooding and pipe surcharge even for short return periods, reaching the full capacity of the sewer system and producing very similar peak flow rates at its outlet. In other words, the shape of the hydrographs resembled the pattern of rainfall intensities up to the point when the capacity of the sewer system was reached, after which peak flows equalled the maximum flow rate allowed by its geometry. Still, higher return periods resulted in higher flow rates at the rising and receding limbs of the hydrograph and, consequently, greater runoff volumes at the outlet of the catchment. The return period had to increase up to 10 years to produce the same effect in the stationary scenario, which demonstrated the importance of considering the effect of CC and the increase in drainage capacity required by RCPs. Consequently, future drainage designs should be adapted to the high water volumes and flows involved by changing climate. Measures to compensate these impacts might consist of increasing the size of sewers and/or implementing Sustainable Drainage Systems (SuDS), which have also been found to provide additional benefits in terms of CC, such as carbon sequestration, mitigation of the Urban Heat Island effect and urban cooling (Charlesworth, 2010).

## 4. Conclusions

This paper developed, applied and validated a methodology to evaluate the response of urban catchments to extreme rainfall events produced by CC using optimized stormwater simulation models. This optimization process, which was developed under the assumption of stationary precipitation using DOE, enabled the design of a reliable statistics-based CC methodology for the projection of future severe storms under RCP scenarios. The results obtained through the application of these methods to a Finnish urban catchment demonstrated its validity to model real case studies. The mathematical and statistical foundations on which the methods were based, as well as the consistent morphologic and climate relationships that supported the results, guaranteed the reliability of the proposed framework for modelling the water balance of new urban environments under the effects of CC, in order to enhance the resilience of cities to flooding phenomena produced by extreme rainfall events.

The results achieved provided evidence of the reliability and precision of the DOE-based methodology to model a real urban catchment. The combination of factorial and response surface designs proved to be capable of both identifying the most influential parameters on the response of the catchment and maximizing the fit between observed and monitored discharge values. The desirability function approach enabled the jointly optimization of three different goodness-of-fit measures, which guaranteed the accuracy of the calibrated catchment parameters. Moreover, the measures of dispersion proposed to characterize CC variables were found to be suitable for representing both their central and extreme values throughout a year, which ensured their usefulness for building multiple regression models to predict AMDP at local weather stations. The results derived from these models reached high coefficients of determination and met the four hypotheses related to their residuals, which validated them for making new estimates. Furthermore, they were based on physical relationships between the CC variables and the values of extreme precipitation, which certified their legitimacy in the future.

The hydrographs obtained for the CC scenarios according to the calibrated catchment parameters resulted in an important increase in both peak flow and volume in relation to the stationary situation. As a result, the probability of flood risk throughout a year increased up to five times when considering the effects of CC, which highlighted the importance of developing accurate and reliable hydrological modelling methodologies to adapt urban drainage designs to the increasingly demanding challenges posed by CC. Therefore, the findings of this research can help to better design drainage strategies to ensure that cities become more resilient to alterations in climate patterns. The flexibility of the methodology, which consists of two interacting modules, further increases its ap-

plicability and enables its stepwise implementation either in isolation or as part of different wholes. Although the validity of the proposed methodology is not limited by the location of the case study, further research should focus on its implementation to other urban catchments with different sizes, drainage systems and weather patterns. Besides, the simulation and analysis of the impact of SuDS on the response of urban catchments under non-stationary extreme rainfall events, as well as the simplification of the integration of DOE in the calibration of stormwater models, are identified as the two other main future line of research to explore in the future.

## Acknowledgments

This paper was possible thanks to the research projects RHIVU (Ref. BIA2012-32463) and SUPRIS-SURReS (Ref. BIA2015-65240-C2-1-R MINECO/FEDER, UE), financed by the Spanish Ministry of Economy and Competitiveness with funds from the State General Budget (PGE) and the European Regional Development Fund (ERDF). The authors wish to express their gratitude to all the entities that provided the data necessary to develop this research: Helsinki Region Environmental Services Authority HSY, Map Service of Espoo, National Land Survey of Finland, Geological Survey of Finland, EURO-CORDEX and European Climate Assessment & Dataset.

## References

- Abdo, K.S., Fiseha, B.M., Rientjes, T.H.M., Gieske, A.S.M., Haile, A.T., 2009. Assessment of climate change impacts on the hydrology of Gilgel Abay catchment in Lake Tana basin, Ethiopia. *Hydrological Processes* 23, 3661-3669.
- Ahrens, D., Samson, P., 2011a. Air Masses and Fronts, in Pople, L., Warde, J., Arvin, S., Chiapella, K., Brady, A. (Eds.), *Extreme Weather and Climate*. Brooks/Cole, Belmont, California (U.S.), pp. 236-267.
- Ahrens, D., Samson, P., 2011b. Wind Systems, in Pople, L., Warde, J., Arvin, S., Chiapella, K., Brady, A. (Eds.), *Extreme Weather and Climate*. Brooks/Cole, Belmont, California (U.S.), pp. 206-235.
- Anderson, T.W., Darling, D.A., 1954. A Test of Goodness of Fit. *Journal of the American Statistical Association* 49, 765-769.
- Aparicio, F.J., 1997. *Fundamentos De Hidrología De Superficie*. Limusa, Mexico City (Mexico).
- ArcGIS for Desktop, 2013. Environmental Systems Research Institute (ESRI), Redlands, California (U.S.).
- ASCE, 1992. *Design and Construction of Urban Stormwater Management Systems*. ASCE and Water Environment Federation, New York (U.S.).
- ASCE, 1982. *Gravity Sanitary Sewer Design and Construction*. ASCE, New York (U.S.).

- [Barco, J., Wong, K.M., Stenstrom, M.K., 2008. Automatic calibration of the U.S. EPA SWMM model for a large urban catchment. \*Journal of Hydraulic Engineering\* 134, 466-474.](#)
- [Bayon, J.R., Jato-Espino, D., Blanco-Fernandez, E., Castro-Fresno, D., 2015. Behaviour of geotextiles designed for pervious pavements as a support for biofilm development. \*Geotextiles and Geomembranes\* 43, 139-147.](#)
- Campos Aranda, D.F., 1998. *Procesos Del Ciclo Hidrológico*, 3 ed. Universidad Autónoma de San Luis Potosí, San Luis Potosí (Mexico).
- Chapin, F.S., Matson, P.A., Mooney, H.A., 2011. Earth's Climate System, in Chapin, M.C. (Ed.), *Principles of Terrestrial Ecosystem Ecology*, 2 ed. Springer, New York (U.S.), pp. 23-62.
- [Charles, S.P., Bari, M.A., Kitsios, A., Bates, B.C., 2007. Effect of GCM bias on downscaled precipitation and runoff projections for the Serpentine catchment, Western Australia. \*International Journal of Climatology\* 27, 1673-1690.](#)
- [Charlesworth, S.M., 2010. A review of the adaptation and mitigation of global climate change using sustainable drainage in cities. \*Journal of Water and Climate Change\* 1, 165-180.](#)
- Chow, V.T., Maidment, D.R., Mays, L.W., 1988. *Applied Hydrology*. McGraw-Hill, New York (U.S.).
- Cronshey, R., McCuen, R.H., Miller, N., Rawls, R., Robbins, S., Woodward, D., 1986. *Urban Hydrology for Small Watersheds*. U. S. Department of Agriculture (USDA) TR-55, 13-21.
- [Derringer, G., Suich, R., 1980. Simultaneous Optimization of Several Response Variables. \*Journal of Quality Technology\* 12, 214-219.](#)
- [Dibike, Y.B., Coulibaly, P., 2005. Hydrologic impact of climate change in the Saguenay watershed: Comparison of downscaling methods and hydrologic models. \*Journal of Hydrology\* 307, 145-163.](#)
- [Dongquan, Z., Jining, C., Haozheng, W., Qingyuan, T., Shangbing, C., Zheng, S., 2009. GIS-based urban rainfall-runoff modeling using an automatic catchment-discretization approach: A case study in Macau. \*Environmental Earth Sciences\* 59, 465-472.](#)
- [Durbin, J., Watson, G.S., 1950. Testing for serial correlation in least squares regression. I. \*Biometrika\* 37, 409-428.](#)
- [Durbin, J., Watson, G.S., 1951. Testing for serial correlation in least squares regression. II. \*Biometrika\* 38, 159-177.](#)
- espoo.fi, Last accessed: May 2016. Map Service. [kartat.espoo.fi/IMS/en/Map](http://kartat.espoo.fi/IMS/en/Map).
- Fisher, R.A., 1925. *Statistical Methods for Research Workers*. Cosmo Publications, New Delhi (India).
- Fowler, H.J., Blenkinsop, S., Tebaldi, C., 2007. Linking climate change modelling to impacts studies: Recent advances in downscaling techniques for hydrological modelling. *International Journal of Climatology* 27, 1547-1578.

- Giorgi, F., Jones, C., Asrar, G.R., 2009. Addressing climate information needs at the regional level: the CORDEX framework. *World Meteorological Organization Bulletin* 58, 175-183.
- Glickman, T.S., 2000. *Glossary of Meteorology*, 2 ed. American Meteorological Society, Boston, Massachusetts (U.S.).
- Gómez Valentín, M., 2007. Información de lluvia a utilizar. Lluvia de proyecto, in Gómez Valentín, M., Dolz Ripollés, J., López Alonso, R., Nanía Escobar, L., Sánchez Tuerros, H., Malgrat, P., Russo, B., Suñer, D., Concha Jopia, R. (Eds.), *Hidrología Urbana*. FLUMEN Institute, Barcelona (Spain), pp. 33-70.
- Guan, M., Sillanpää, N., Koivusalo, H., 2015. Modelling and assessment of hydrological changes in a developing urban catchment. *Hydrological Processes* 29, 2880-2894.
- Hassan, M., Du, P., Jia, S., Iqbal, W., Mahmood, R., Ba, W., 2015. An assessment of the South Asian summer monsoon variability for present and future climatologies using a high resolution regional climate model (RegCM4.3) under the AR5 scenarios. *Atmosphere* 6, 1833-1857.
- Hirsch, R.M., Helsel, D.R., Cohn, T.A., Gilroy, E.J., 1993. *Statistical Analysis of Hydrologic Data*, in Maidment, D.R. (Ed.), *Handbook of Hydrology*. McGraw-Hill, New York (U.S.), pp. 1-55.
- Houghton, J.C., 1978. Birth of a parent: The Wakeby Distribution for modeling flood flows. *Water Resources Research* 14, 1105-1109.
- Huntington, T.G., 2006. Evidence for intensification of the global water cycle: Review and synthesis. *Journal of Hydrology* 319, 83-95.
- IPCC, 2007. *Climate Change 2007: The Physical Science Basis*. Cambridge University Press, Cambridge (U.K.) and New York (U.S.).
- Jain, S.K., Sudheer, K.P., 2008. Fitting of hydrologic models: A close look at the nash-sutcliffe index. *Journal of Hydrologic Engineering* 13, 981-986.
- Jato-Espino, D., Charlesworth, S.M., Bayon, J.R., Warwick, F., 2016. Rainfall-runoff simulations to assess the potential of SuDS for mitigating flooding in highly urbanized catchments. *International Journal of Environmental Research and Public Health* 13, 149.
- Jenson, S.K., Domingue, J.O., 1988. Extracting topographic structure from digital elevation data for geographic information system analysis. *Photogrammetric Engineering and Remote Sensing* 54, 1593-1600.
- Kay, A.L., Rudd, A.C., Davies, H.N., Kendon, E.J., Jones, R.G., 2015. Use of very high resolution climate model data for hydrological modelling: baseline performance and future flood changes. *Climatic Change* 133, 193-208.
- Kleinn, J., Frei, C., Gurtz, J., Lüthi, D., Vidale, P.L., Schär, C., 2005. Hydrologic simulations in the Rhine basin driven by a regional climate model. *Journal of Geophysical Research D: Atmospheres* 110, 1-18.

- Knebl, M.R., Yang, Z.-., Hutchison, K., Maidment, D.R., 2005. Regional scale flood modeling using NEXRAD rainfall, GIS, and HEC-HMS/ RAS: A case study for the San Antonio River Basin Summer 2002 storm event. *Journal of Environmental Management* 75, 325-336.
- Korhonen, J., Kuusisto, E., 2010. Long-term changes in the discharge regime in Finland. *Hydrology Research* 41, 253-268.
- Krebs, G., Kokkonen, T., Valtanen, M., Koivusalo, H., Setälä, H., 2013. A high resolution application of a stormwater management model (SWMM) using genetic parameter optimization. *Urban Water Journal* 10, 394-410.
- Kundzewicz, Z.W., Schellnhuber, H.-., 2004. Floods in the IPCC TAR perspective. *Natural Hazards* 31, 111-128.
- Levene, H., 1960. Robust Tests for Equality of Variances, in Olkin, I. (Ed.), *Contributions to Probability and Statistics*. Stanford University Press, Palo Alto (California), pp. 278-293.
- Lindström, G., Bergström, S., 2004. Runoff trends in Sweden 1807-2002. *Hydrological Sciences Journal* 49, 69-84.
- Matveev, L.T., Matveev, Y.L., 2009. Formation of Precipitation, in Shiklomanov, I.A. (Ed.), *Hydrological Cycle*, 2 ed. Eolss Publishers Co. Ltd., Oxford (U.K.), pp. 176-192.
- McCuen, R.H., Johnson, P., Ragan, R., 1996. *Highway Hydrology: Hydraulic Design Series*, 2 ed. Federal Highway Administration, Washington, D.C. (U.S.).
- Menzhulin, G.V., 2009. Transpiration, in Shiklomanov, I.A. (Ed.), *Hydrological Cycle*, 2 ed. Eolss Publishers Co. Ltd., Oxford (U.K.), pp. 163-175.
- Minitab 17 Statistical Software, 2014. Minitab, Inc., State College, Pensilvania (U.S.).
- Mockus, V., 1964. Hydrology, in *Anonymous National Engineering Handbook*. United States Geological Survey (USGS), Gainesville, Florida (U.S.), pp. 1-24.
- Montgomery, D.C., 2004. *Diseño Y Análisis De Experimentos*, 2 ed. Limusa Wiley, Mexico City (Mexico).
- Moss, R., Babiker, M., Brinkman, S., Calvo, E., Carter, T., Edmonds, J., Elgizouli, I., Emori, S., Erda, L., Hibbard, K., Jones, R., Kainuma, M., Kelleher, J., Lamarque, J.F., Manning, M., Matthews, B., Meehl, J., Meyer, L., Mitchell, J., Nakicenovic, N., O'Neill, B., Pichs, R., Riahi, K., Rose, S., Runci, P., Stouffer, R., van Vuuren, D., Weyant, J., Wilbanks, T., van Ypersele, J.P., Zurek, M., 2008. *Towards New Scenarios for Analysis of Emissions, Climate Change, Impacts, and Response Strategies*. Intergovernmental Panel on Climate Change Technical Summary, 5-25.
- Nash, J.E., Sutcliffe, J.V., 1970. River flow forecasting through conceptual models part I - A discussion of principles. *Journal of Hydrology* 10, 282-290.
- NRCS, 2015. Part 630 – Hydrology, in *National Engineering Handbook*. U.S. Department of Agriculture (USDA), Washington, D.C. (U.S.).

- NLS, Last accessed: May 2016. National Land Survey of Finland - File service of open data. [tiedostopalvelu.maanmittauslaitos.fi/tp/kartta?lang=en](http://tiedostopalvelu.maanmittauslaitos.fi/tp/kartta?lang=en) .
- Ouyang, F., Zhu, Y., Fu, G., Lü, H., Zhang, A., Yu, Z., Chen, X., 2015. Impacts of climate change under CMIP5 RCP scenarios on streamflow in the Huangnizhuang catchment. *Stochastic Environmental Research and Risk Assessment* 29, 1781-1795.
- Perales-Momparler, S., Andrés-Doménech, I., Andreu, J., Escuder-Bueno, I., 2015. A regenerative urban stormwater management methodology: The journey of a Mediterranean city. *Journal of Cleaner Production* 109, 174-189.
- Pumo, D., Caracciolo, D., Viola, F., Noto, L.V., 2016. Climate change effects on the hydrological regime of small non-perennial river basins. *Science of the Total Environment* 542, 76-92.
- Qin, H.-., Li, Z.-., Fu, G., 2013. The effects of low impact development on urban flooding under different rainfall characteristics. *Journal of Environmental Management* 129, 577-585.
- Rossman, L., 2010. Storm Water Management Model User's Manual - Version 5.0. U.S. Environmental Protection Agency, Cincinnati (U.S.).
- Shapiro, S.S., Wilk, M.B., Chen, H.J., 1968. A Comparative Study of Various Tests for Normality. *Journal of the American Statistical Association* 63, 1343-1372.
- Schwab, D.J., Beletsky, D., 2003. Relative effects of wind stress curl, topography, and stratification on large-scale circulation in Lake Michigan. *Journal of Geophysical Research C: Oceans* 108, 26-1.
- Shao, Q., Wong, H., Xia, J., Ip, W.-., 2004. Models for extremes using the extended three-parameter Burr XII system with application to flood frequency analysis. *Hydrological Sciences Journal* 49, 685-701.
- Sillanpää, N., 2013. Effects of Suburban Development on Runoff Generation and Water Quality. Aalto University School of Engineering, Espoo (Finland).
- Sillanpää, N., Koivusalo, H., 2015. Impacts of urban development on runoff event characteristics and unit hydrographs across warm and cold seasons in high latitudes. *Journal of Hydrology* 521, 328-340.
- Sloat, M.S., Hwang, R.B., 1989. Sensitivity study of detention basins in urbanized watershed. *Journal of Urban Planning and Development* 115, 135-155.
- Stephens, M.A., 1974. EDF Statistics for Goodness of Fit and Some Comparisons. *Journal of the American Statistical Association*. 69, 730-737.
- Stevens, J.P., 2009. *Applied Multivariate Statistics for the Social Sciences*, 5 ed. Taylor & Francis, New York (U.S.).
- SWMM 5.1.010, 2015. United States Environmental Protection Agency (U.S. EPA), Washington, D.C. (U.S.).
- Tabachnick, B.G., Fidell, L.S., 1989. *Using Multivariate Statistics*, 2 ed. Harper Collins, New York (U.S.).

- Tarboton, D.G., Bras, R.L., Rodriguez-Iturbe, I., 1991. On the extraction of channel networks from digital elevation data. *Hydrological Processes* 5, 81-100.
- Témez, J.R., 1978. *Cálculo Hidrometeorológico De Caudales Máximos En Pequeñas Cuencas Naturales*. MOPU, Madrid (Spain).
- Temprano, J., Arango, Ó, Cagiao, J., Suárez, J., Tejero, I., 2006. Stormwater quality calibration by SWMM: A case study in Northern Spain. *Water SA* 32, 55-63.
- Valtanen, M., Sillanpää, N., Setälä, H., 2014. Effects of land use intensity on stormwater runoff and its temporal occurrence in cold climates. *Hydrological Processes* 28, 2639-2650.
- Veijalainen, N., 2012. *Estimation of Climate Change Impacts on Hydrology and Floods in Finland*. Aalto University School of Engineering, Espoo (Finland).
- Wang, X., Yang, T., Krysanova, V., Yu, Z., 2015. Assessing the impact of climate change on flood in an alpine catchment using multiple hydrological models. *Stochastic Environmental Research and Risk Assessment* 29, 2143-2158.
- Whipple, W., Grigg, N.S., Grizzard, T., Randall, C.W., Shubinski, R.P., Tucker, L.S., 1982. *Stormwater Management in Urbanizing Areas*. Prentice Hall, New Jersey (U.S.).
- Wilson, D., Hisdal, H., Lawrence, D., 2010. Has streamflow changed in the Nordic countries? - Recent trends and comparisons to hydrological projections. *Journal of Hydrology* 394, 334-346.
- Woodward, D.E., Hawkins, R.H., Jiang, R., Hjelmfelt Jr., A.T., Van Mullem, J.A., Quan, Q.D., 2003. Runoff curve number method: Examination of the initial abstraction ratio. *World Water and Environmental Resources Congress*, 691-700.
- Zhang, X., Zwiers, F.W., Hegerl, G.C., Lambert, F.H., Gillett, N.P., Solomon, S., Stott, P.A., Nozawa, T., 2007. Detection of human influence on twentieth-century precipitation trends. *Nature* 448, 461-465.
- Zoppou, C., 2001. Review of urban storm water models. *Environmental Modelling and Software* 16 (2001), 195-231.